applied sciences

MDPI

Article

Analysis and Reduction of Nonlinear Effects in Optical Fiber Frequency Transfer

Jing Gao [1,2,†], Linbo Zhang [1,2,†], Dongdong Jiao [1,2], Guanjun Xu [1,2,*], Jiayu Bu [1,2], Mengfan Wu [1,2], Qi Zang [1,2], Xiang Zhang [1,2], Ruifang Dong [1,2,*], Tao Liu [1,2,*] and Shougang Zhang [1,2]

1 National Time Service Center, Chinese Academy of Sciences, 3 East Shuyuan Road, Xi'an 710600, China; gaojing@ntsc.ac.cn (J.G.); jiaodd@ntsc.ac.cn (D.J.); bujiayu@ntsc.ac.cn (J.B.)

2 Key Laboratory of Time and Frequency Standards, Chinese Academy of Sciences, 3 East Shuyuan Road, Xi'an 710600, China

* Correspondence: xuguanjun@ntsc.ac.cn (G.X.); dongruifang@ntsc.ac.cn (R.D.); taoliu@ntsc.ac.cn (T.L.)

† These authors contributed equally to this work.

Abstract: Nonlinear effects in optical fiber frequency transfer have a significant impact on the precision of frequency transfer. We investigate the main nonlinear effects, including the Brillouin scattering and the Raman scattering, in optical fiber frequency transfer through theoretical and simulation calculations in detail. The calculation results show that the threshold powers of the Brillouin scattering and the Raman scattering decrease with the increase in the fiber length; however, the fiber length has little to no impact on the threshold powers when the fiber length is greater than 10 km. The threshold powers, including the Brillouin scattering and the Raman scattering, increase as the attenuation coefficient increases. Conversely, when it comes to the gain coefficients, the outcomes exhibit a reverse trend. When the linewidth Δv_{laser} of the laser source is from 1 Hz to 1 MHz, the linewidth Δv_{laser} does not affect the threshold powers of the Brillouin scattering. This study seeks to offer design guidance aimed at mitigating nonlinear effects in optical fiber frequency transfer. The calculated results hold considerable potential in guiding various applications reliant on Brillouin and Raman scattering properties, such as laser technology and optical fiber sensing.

Keywords: optical fiber frequency transfer; nonlinear effects; Brillouin scattering; Raman scattering; optical clock

Citation: Gao, J.; Zhang, L.; Jiao, D.; Xu, G.; Bu, J.; Wu, M.; Zang, Q.; Zhang, X.; Dong, R.; Liu, T.; et al. Analysis and Reduction of Nonlinear Effects in Optical Fiber Frequency Transfer. *Appl. Sci.* **2023**, *13*, 12762. https://doi.org/10.3390/app132312762

Academic Editor: Dong Hou

Received: 13 October 2023
Revised: 13 November 2023
Accepted: 18 November 2023
Published: 28 November 2023

1. Introduction

In recent years, the achievement of precision levels at 10^{-18} and the remarkable stability of optical clocks have played a significant role in various research domains, including navigation, fundamental physics, applied research, chronometric geodesy, and the quest for dark matter [1–6]. The evolution of optical clocks has given rise to high-precision optical frequency transfer methods. Fiber optic links have demonstrated exceptional performance in transmitting optical frequencies with instabilities as low as 10^{-20} over distances spanning hundreds to thousands of kilometers [7–13].

To accomplish remote optical clock frequency comparisons and enable long-distance frequency reference distribution, there has been significant interest and comprehensive research focused on high-precision optical frequency transfer through communication fibers [7–10]. However, the transmission of signals in optical fibers is affected by nonlinear effects, including Brillouin scattering, Raman scattering, and Rayleigh scattering, which can cause additional noise in the optical fiber link, thereby affecting transmission performance [14–18]. Nonlinear effects not only introduce noise into the optical fiber frequency transfer system but also result in a form of nonlinear loss of the signal, thus limiting the increase in input fiber power and reducing the optical signal-to-noise ratio of the optical fiber frequency transfer system, thereby severely constraining the improvement of transmission system performance [19–22]. Simultaneously, when the laser power injected into the optical fiber exceeds the threshold power of the scattering, the scattering occurs [19,23]. Scattering primarily affects the system by causing crosstalk between channels and energy loss in the channels. The Brillouin frequency shift is approximately 10~11 GHz at 1550 nm. When the channel spacing of the system matches the Brillouin frequency shift, it leads to crosstalk between the channels [24]. Additionally, because scattering causes some channel power to be transferred to noise, it affects power amplification.

Although there have been numerous studies on the threshold power of Brillouin scattering and Raman scattering in the context of laser and optical fiber sensing [20,24–28], there is a relative scarcity of research on fiber optical frequency transfer, particularly in long-distance and high-precision transmission [7,11–13]. Existing studies primarily focus on estimating the threshold power for generating Brillouin scattering and Raman scattering using the optical fiber length while neglecting other important parameters, such as the attenuation coefficient and the gain coefficient. With the growing demand for large-scale scientific research projects, like the "high precision ground-based timing system" in the national major scientific and technological infrastructure plan [12,13], it becomes crucial to investigate the impact of multiple parameters on the threshold power for generating Brillouin scattering and Raman scattering. This is because the parameters of optical fibers used in long-distance transmission differ from those in laboratory settings. For instance, the attenuation coefficient of optical fibers in the field is influenced by various factors, such as vibration and temperature, which differs from the attenuation coefficient in the laboratory and affects the estimation of the threshold power for generating Brillouin scattering and Raman scattering. Therefore, it is imperative to conduct a detailed study on the influence of multiple parameters on the threshold power for generating Brillouin scattering and Raman scattering in the context of long-distance and high-precision field optical fiber frequency transfer.

In this study, we comprehensively investigate nonlinear effects in optical fiber frequency transfer through theoretical and simulation calculations. We specifically focus on two primary nonlinear effects: Brillouin scattering and Raman scattering. Generally, the threshold power for Brillouin scattering is two orders of magnitude lower than that for Raman scattering. Our calculations reveal that the threshold powers for both Brillouin and Raman scattering decrease with increasing fiber length. However, these threshold powers remain relatively constant when the fiber length exceeds 10 km. When the fiber length L is kept constant, the threshold power for both Brillouin and Raman scattering decreases as the gain coefficients increase. Conversely, this trend reverses for the attenuation coefficient. Furthermore, when the fiber length is predetermined, and the linewidth of the laser source ranges from 1 Hz to 1 MHz, the linewidth of the laser source does not impact the threshold powers required to generate Brillouin scattering. To the best of our knowledge, this study represents the first comprehensive exploration of nonlinear effects with multiple parameters in optical fiber frequency transfer. Our work aims to offer valuable design guidance for mitigating nonlinear effects in optical fiber frequency transfer and, in particular, long-distance and high-precision field fiber optical frequency transmission. The calculation results hold significant potential for guiding various applications utilizing Brillouin and Raman scattering characteristics, such as laser technology and optical fiber sensing.

This paper is structured as follows. We present the fundamental principle, including the high-precision optical frequency signal transmission, the Brillouin scattering, and the Raman scattering, in Section 2. In Section 3, the calculation results of the threshold powers for the Brillouin scattering and the Raman scattering, including the forward and backward scattering, are presented. The conclusions are summarized in Section 4.

2. Fundamental Principle

Figure 1 illustrates the system schematic of high-precision optical frequency signal transmission based on a fiber optic link. The optical frequency signal is generated by a laser that can output continuous laser light and is injected into the fiber optic link. At the transmitter end of the system, the optical signal is split into two paths, with one path serving as the reference light and the other path being modulated by Bi-Actuator 1 before being transmitted through the fiber optic link to the remote end, where it is further modulated by Bi-Actuator 2. At the remote end, a portion of the optical signal is reflected back to the transmitter end by a reflective mirror along the same path, while another portion is provided to the user. The light that is reflected back and the reference light at the transmitter end undergo beat frequency comparison to extract phase noise information introduced by the transmission system. This information is then subjected to noise suppression through a noise feedback control system to ensure that the transmitted light at the user end exhibits the same characteristics as the light source.

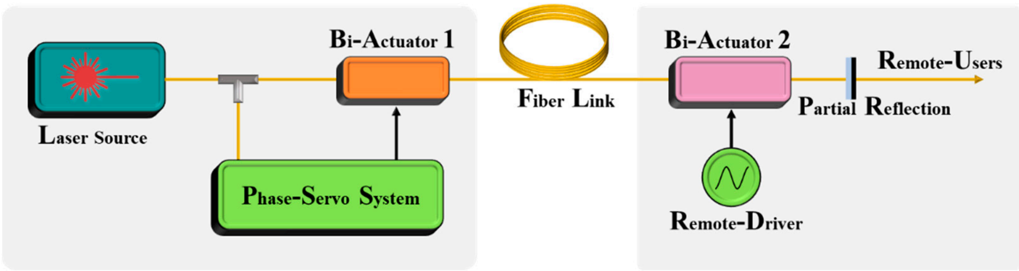

Figure 1. Schematic of the basic principle of optical frequency transmission via fiber with the active phase-noise compensation system. Laser Source and Phase-Servo System represent continuous laser light and the active phase-noise compensation system, respectively. Bi-Actuator denotes bidirectional modulator.

As shown in Figure 2, laser signals transmitted in optical fibers can result in nonlinear effects due to non-elastic collisions [24,29,30]. Depending on the optical intensity, two different nonlinear effects can occur: stimulated Raman scattering and stimulated Brillouin scattering. Both of these nonlinear effects are intensity dependent, but the optical intensity threshold for stimulated Brillouin scattering is significantly lower compared to Raman scattering. Even at lower power levels, Brillouin scattering can occur spontaneously, as it is driven by the scattering of phonons generated thermally. Higher input optical power leads to the generation of a large number of phonons, and when two counter-propagating optical waves in the fiber intersect, they create a moving refractive index grating. The greater the reflected optical power, the stronger the grating, resulting in higher effective reflectivity. When the incident optical power exceeds a certain threshold, stimulated Brillouin phonons can scatter a significant portion of the incident optical power back to the input end of the optical fiber. For silica optical fibers, the material itself exhibits relatively weak nonlinear effects, but the combination of a small effective mode area and long propagation length in the optical fiber greatly enhances these nonlinear effects.

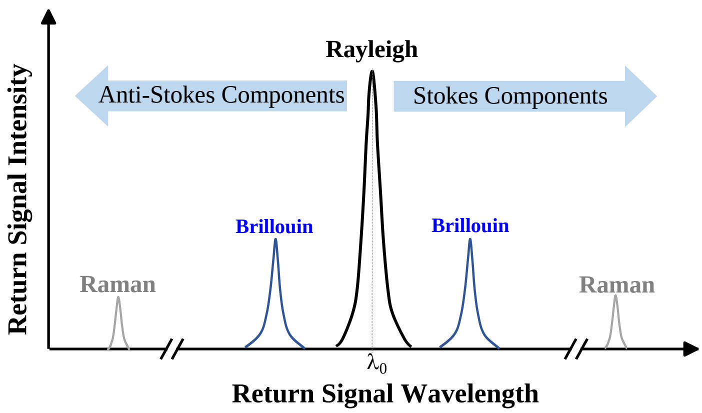

Figure 2. Schematic of the basic principle of nonlinear effects in optical fiber frequency transfer [31]. λ_0 is the center wave length of the transmitted light.

The frequency of the reflected beam generated by stimulated Brillouin scattering is slightly lower than that of the incident beam. It corresponds to the frequency v_B of phonons, and the corresponding frequency shift is called the Brillouin frequency shift. The frequency shift is determined by the phase matching condition, and it can be calculated using the refractive index n, the speed of sound v_a = 6 × 10^3 m/s, and the vacuum wavelength λ_0. The frequency v_B can be expressed as [24,32,33]:

$$v_B = \frac{2nv_a}{\lambda_0} \tag{1}$$

The Brillouin frequency shift depends on the material composition and, to some extent, the temperature and pressure of the medium. For silica optical fibers, the Brillouin frequency shift is approximately 11 GHz. The intrinsic bandwidth of Brillouin gain is typically between 10 and 100 MHz, and the linewidth Δv_B is determined by the phonon lifetime t, where $\Delta v_B = 1/2\pi t$. In theory, phonon absorption leads to a shorter phonon lifetime and thus a narrower linewidth. However, the bandwidth of Brillouin gain is significantly broadened due to various influences, such as lateral variations in sound velocity or longitudinal temperature changes.

The threshold power P_{crit-B} for Brillouin stimulated scattering is given by [24,32,33]:

$$\begin{cases} P_{crit-B} = \frac{21A_{eff}}{\gamma_B L_{eff}}\left(1+\frac{\Delta v_{laser}}{\Delta v_B}\right) \\ A_{eff} = \frac{\left(\iint_{-\infty}^{\infty}|F(x,y)|^2 dxdy\right)^2}{\iint_{-\infty}^{\infty}|F(x,y)|^4 dxdy} \\ L_{eff} = \frac{1-e^{-\alpha L}}{\alpha} \end{cases} \tag{2}$$

where A_{eff} is the effective mode area of the fiber and γ_B is the gain coefficient of the Brillouin scattering. $F(x,y)$ represents the transverse distribution inside the core of the optical fiber. L_{eff} denotes the effective gain length of the optical fiber. α and L are the attenuation coefficient and length of the optical fiber. Δv_{laser} is the linewidth of the laser source.

In optical fiber transmission, Raman scattering can negatively impact performance. Similar to Brillouin scattering, the generation of Raman scattering also has an obvious threshold. Under equivalent conditions, the threshold power for generating Raman scattering is approximately two orders of magnitude higher than the threshold power of Brillouin scattering [24]. In general, Raman scattering includes forward Raman scattering and backward Raman scattering. The threshold power $P_{crit-R-B}$ for generating backward Raman scattering is about 25% higher than the threshold power $P_{crit-R-F}$ for generating forward Raman scattering. Based on the classical estimation theory of the threshold power for generating Raman scattering, the threshold power $P_{crit-R-F}$ for generating forward Raman scattering and the threshold power $P_{crit-R-B}$ for generating backward Raman scattering can be expressed as [24,32,33]

$$\begin{cases} P_{crit-R-F} = \frac{16A_{eff}}{\gamma_R L_{eff}} \\ P_{crit-R-B} = \frac{20A_{eff}}{\gamma_R L_{eff}} \end{cases} \tag{3}$$

where γ_R is the gain coefficient of the Raman scattering.

3. Simulation and Results

In the simulation and calculation of the threshold power for generating Brillouin scattering and Raman scattering, we consider an optical fiber made of fused silica single mode fiber with a refractive index of 1.451 and a light wavelength of 1.5 µm. The Brillouin frequency shift is estimated to be around 11 GHz.

3.1. Stimulated Brillouin Scattering

According to Equation (2), we assess the threshold power of generating the Brillouin scattering as a function of the optical fiber's length L with the various effective mode area A_{eff}, including 1 × 10^{-11} m^2, 5 × 10^{-11} m^2, and 1 × 10^{-10} m^2. The corresponding results for the threshold power P_{crit-B} are presented in Figure 3.

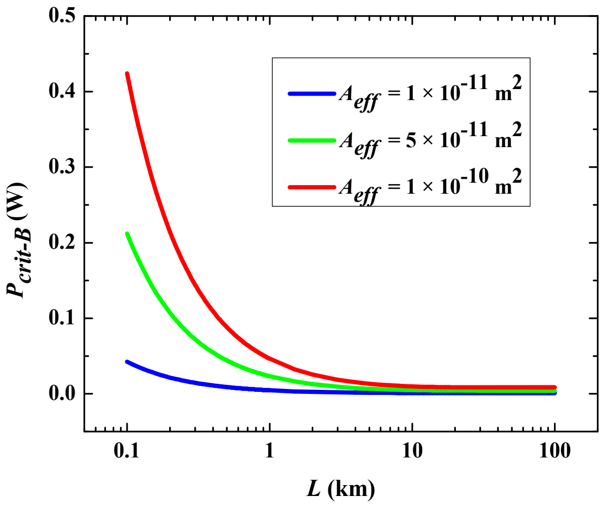

Figure 3. The threshold power P_{crit-B} for generating the Brillouin scattering as a function of the length L of the optical fiber. The attenuation coefficient of the optical fiber α is 0.2 dB/km. The linewidth Δv_{laser} of the laser source and the linewidth Δv_B of the Brillouin scattering are 1 kHz and 10 MHz, respectively. The gain coefficient γ_B of the Brillouin scattering is 5×10^{-11} m/W.

In general, for fiber lengths of less than 1 km, the threshold power P_{crit-B} typically falls in the range of 100 mW. However, for fiber lengths ranging from 1 km to 100 km, the threshold powers for Brillouin scattering are typically around 10 mW. When the effective mode area A_{eff} of the fiber remains constant, the threshold powers for Brillouin scattering decrease as the fiber length increases. For instance, at fiber lengths of 100 m and 500 m, the threshold powers for Brillouin scattering with an effective mode area of 1×10^{-10} m^2 are approximately 424 mW and 88 mW, respectively. Conversely, when the fiber length exceeds 10 km, the threshold power P_{crit-B} remains relatively constant. Specifically, it hovers around 1 mW for an effective mode area A_{eff} of 1×10^{-11} m^2, approximately 4 mW for A_{eff} of 5×10^{-11} m^2, and about 8 mW for A_{eff} of 1×10^{-10} m^2. These calculations hold potential theoretical significance for guiding laser and optical fiber sensing applications that utilize Brillouin scattering characteristics. Additionally, when the fiber length L is held constant, the threshold powers for Brillouin scattering increase with a larger effective mode area A_{eff} of the fiber. For instance, at a fixed fiber length of 2 km, the threshold powers for Brillouin scattering with effective mode areas A_{eff} of 1×10^{-11} m^2, 5×10^{-11} m^2, and 1×10^{-10} m^2 are approximately 2.6 mW, 12.7 mW, and 25.5 mW, respectively.

In Figure 4a, we present the threshold power P_{crit-B} for generating Brillouin scattering as a function of the attenuation coefficient α of the optical fiber when the laser source linewidth Δv_{laser}, Brillouin scattering linewidth Δv_B, and Brillouin scattering gain coefficient γ_B are set at 1 kHz, 10 MHz, and 5×10^{-11} m/W, respectively. Generally, when the fiber length L is held constant, the threshold powers for Brillouin scattering increase with higher values of the attenuation coefficient α of the optical fiber. For example, at L = 50 km, the threshold powers for α = 0.1 dB/km, α = 1 dB/km, and α = 2 dB/km are approximately 4 mW, 42 mW, and 84 mW, respectively. However, with L = 1 km and α = 0.5 dB/km, the threshold power for Brillouin scattering is approximately 53 mW, which is about 30 mW higher than that for L = 10 km. Interestingly, when α is varied between 0.1 dB/km and 2 dB/km, the threshold power for Brillouin scattering at L = 50 km remains essentially unchanged compared to that at L = 10 km.

The calculation results depicted in Figure 4b present the threshold powers of Brillouin scattering as a function of the Brillouin scattering gain coefficient γ_B. Here, the parameters include the laser source linewidth Δv_{laser} at 1 kHz, Brillouin scattering linewidth Δv_B at 10 MHz, and optical fiber attenuation coefficient α at 0.2 dB/km. Generally, when the fiber length L is constant, the threshold power P_{crit-B} of Brillouin scattering decreases with an increasing Brillouin scattering gain coefficient γ_B. For instance, at L = 1 km, the threshold powers for γ_B values of 1×10^{-11} m/W, 6×10^{-11} m/W, and 1×10^{-10} m/W are approximately 232 mW, 39 mW, and 23 mW, respectively. When γ_B ranges from 1×10^{-11} m/W to 1×10^{-10} m/W, the threshold power of Brillouin scattering remains essentially constant for L = 50 km and L = 10 km. For a fixed L = 10 km and $\gamma_B = 7 \times 10^{-11}$ m/W, the threshold power of Brillouin scattering is approximately 7 mW. This is, notably, 26 mW lower than the corresponding value for L = 1 km.

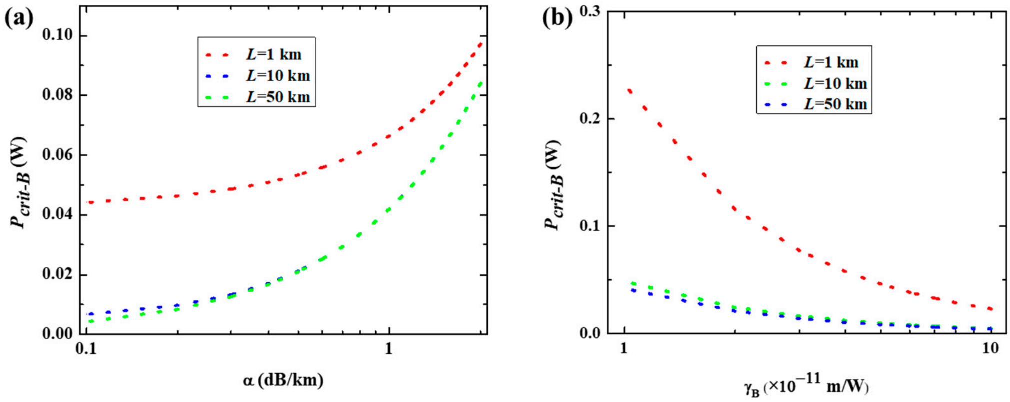

Figure 4. The threshold power P_{crit-B} for generating the Brillouin scattering as a function of the attenuation coefficient α of the optical fiber and the gain coefficient γ_B of the Brillouin scattering. The effective mode area A_{eff} of the fiber is 1×10^{-10} m^2. (**a**) The attenuation coefficient α of the optical fiber. (**b**) The gain coefficient γ_B of the Brillouin scattering.

Figure 5 illustrates the threshold powers required to generate Brillouin scattering as a function of the laser source linewidth Δv_{laser} for different fiber lengths: 1 km, 10 km, and 50 km. Generally, when the fiber length L is fixed and the laser source linewidth Δv_{laser} ranges from 1 Hz to 1 MHz, it does not impact the threshold powers for generating Brillouin scattering. The threshold powers remain approximately 46 mW for L = 1 km, 10 mW for L = 10 km, and 8 mW for L = 50 km, respectively. However, when Δv_{laser} is determined between 1 MHz and 10 MHz with a constant fiber length L, the threshold powers of Brillouin scattering increase proportionally. For instance, at L = 10 km, the threshold powers are approximately 12 mW and 16 mW for Δv_{laser} = 2 MHz and Δv_{laser} = 6 MHz, respectively.

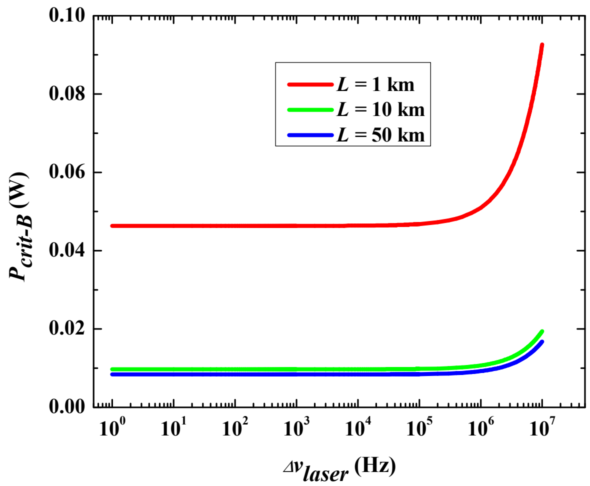

Figure 5. The threshold power P_{crit-B} for generating the Brillouin scattering as a function of the linewidth Δv_{laser} of the laser source. The attenuation coefficient of the optical fiber α is 0.2 dB/km. The linewidth Δv_B of the Brillouin scattering is 10 MHz. The gain coefficient γ_B of the Brillouin scattering is 5×10^{-11} m/W. The effective mode area A_{eff} of the fiber is 1×10^{-10} m^2.

3.2. Raman Scattering

Utilizing Equation (3), we calculate the threshold power P_{crit-R} for generating Raman scattering as a function of the length L of the optical fiber, considering an effective mode area A_{eff} of 1.0×10^{-10} m^2, an attenuation coefficient α of 0.2 dB/km, and a gain coefficient γ_R for Raman scattering of 4.2×10^{-13} m/W. The results of this calculation are illustrated in Figure 6.

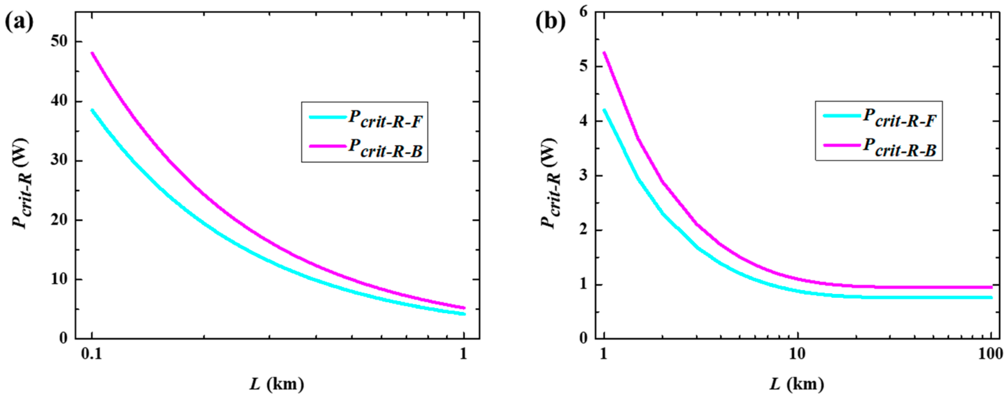

Figure 6. The threshold power for generating the Raman scattering as a function of the length L of the optical fiber. (**a**) The fiber with less than 1 km in length. (**b**) The fiber with the length from 1 km to 100 km.

As shown in Figure 6, when the fiber length L varies from 0.1 km to 1 km, the threshold powers, including $P_{crit-R-B}$ for generating backward Raman scattering and $P_{crit-R-F}$ for generating forward Raman scattering, are consistently in the vicinity of 10 W. This value is roughly two orders of magnitude greater than the threshold powers for Brillouin scattering at the same fiber length. This discrepancy can be attributed to the significantly higher gain coefficient of Brillouin scattering, which is approximately two orders of magnitude larger than the gain coefficient γ_R of Raman scattering. The threshold powers for generating Raman scattering are approximately 1 W for fiber lengths ranging from 1 km to 100 km. In cases where the fiber length L is fixed, $P_{crit-R-B}$ for backward Raman scattering is approximately 25% higher than that for forward Raman scattering. Generally, the threshold powers for Brillouin scattering exhibit a decreasing trend as the fiber length L increases. For instance, for a 0.5 km fiber length, $P_{crit-R-F}$ and $P_{crit-R-B}$ are approximately 8 W and 10 W, respectively, and they decrease by approximately 3.8 W and 4.8 W, respectively, as the fiber length increases. However, for fiber lengths exceeding 10 km, the threshold powers for generating Raman scattering remain relatively constant, paralleling the behavior observed in Brillouin scattering.

When the optical fiber's length is 10 km, Figure 7a displays the calculated threshold powers for generating Raman scattering as a function of the attenuation coefficient α of the optical fiber. It is observed that as the attenuation coefficient α of the optical fiber increases, the threshold powers for generating Raman scattering also increase. For example, when the attenuation coefficients are 1 dB/km and 2 dB/km, the threshold powers for backward Raman scattering are approximately 4.8 W and 9.5 W, respectively, while the threshold powers for forward Raman scattering are approximately 3.8 W and 7.6 W, respectively. Furthermore, when the attenuation coefficient α of the optical fiber remains constant at 0.5 dB/km, the threshold power $P_{crit-R-B}$ for backward Raman scattering surpasses that of forward Raman scattering, with values of about 2.4 W and 1.9 W, respectively.

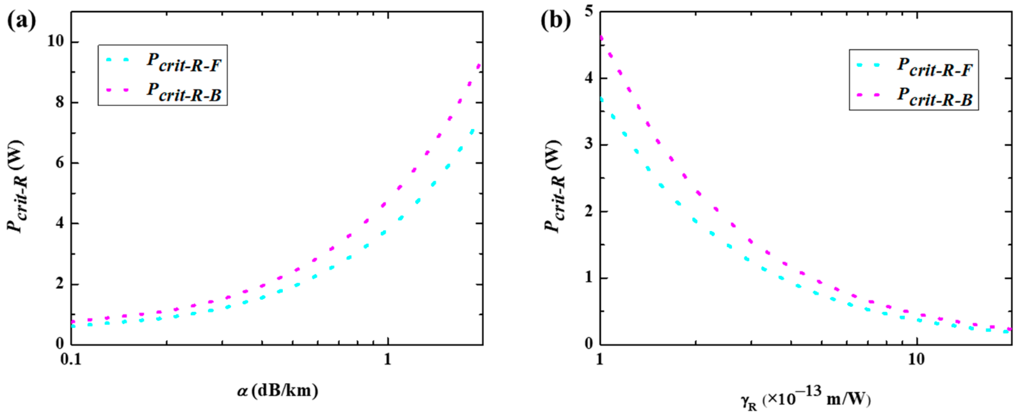

Figure 7. The threshold power for generating the Raman scattering as a function of the attenuation coefficient α of the optical fiber and the gain coefficient γ_R of the Raman scattering. (**a**) The attenuation coefficient α based on the gain coefficient γ_R = 4.2 $\times$ 10^{-13} m/W and the effective mode area A_{eff} = 1.0 $\times$ 10^{-10} m^2. (**b**) The gain coefficient γ_B based on the attenuation coefficient α = 0.2 dB/km and the effective mode area A_{eff} = 1.0 $\times$ 10^{-10} m^2.

As shown in Figure 7b, the threshold powers of the Raman scattering as a function of the gain coefficient γ_B of the Raman scattering are presented, where the length L of the fiber is 10 km. In general, the threshold power P_{crit-R}, including the backward Raman scattering and the forward Raman scattering, decreases as the gain coefficient γ_R of the Raman scattering increases. For instance, consider two scenarios with different gain coefficients for Raman scattering: 1 $\times$ 10^{-13} m/W and 1 $\times$ 10^{-12} m/W, resulting in average threshold powers of approximately 4.2 W and 0.4 W, respectively. When the gain coefficient γ_R for Raman scattering is established, the threshold power $P_{crit-R-F}$ for forward Raman scattering is found to be lower than that for backward Raman scattering. Specifically, with gain coefficients of 5 $\times$ 10^{-13} m/W for Raman scattering, the threshold power for forward Raman scattering is approximately 0.7 W, which is 0.2 W less than that for backward Raman scattering.

In this study, we compare the research on the threshold powers of Brillouin scattering and Raman scattering in high-precision optical fiber frequency transfer with previous works [11–18] (Table 1). However, unlike these works, our study focuses on investigating the Brillouin scattering threshold power and Raman scattering threshold power in detail. We also examine the influence of various parameters on these threshold powers. This research is crucial for long-distance and high-precision fiber optical frequency transfer. For instance, in the "high precision ground-based timing system" of the national major scientific and technological infrastructure plan [12,13], the attenuation coefficient α of the optical fiber in the field differs from the attenuation coefficient in the laboratory, which can impact the threshold powers.

Table 1. Comparison of research on the threshold powers of the Brillouin scattering and Raman scattering in the high-precision optical fiber frequency transfer.

<table>
<tr><th rowspan="2">Item</th><th rowspan="2">Research Team</th><th colspan="4">Brillouin Scattering Threshold Power</th><th rowspan="2">Raman Scattering Threshold Power</th></tr>
<tr><th>L</th><th>γ_B</th><th>α</th><th>Δv_{laser}</th></tr>
<tr><td>1</td><td>Ref. [11]</td><td rowspan="5">Yes</td><td>No</td><td rowspan="5">No</td><td>No</td><td rowspan="4">No</td></tr>
<tr><td>2</td><td>Ref. [18]</td><td>No</td><td>No</td></tr>
<tr><td>3</td><td>Refs. [14,15]</td><td>Yes</td><td>Yes</td></tr>
<tr><td>4</td><td>Refs. [16,17]</td><td>Yes</td><td>No</td></tr>
<tr><td>5</td><td>Refs. [12,13]</td><td>No</td><td>Yes</td><td>Yes</td></tr>
<tr><td>6</td><td>This work</td><td>Yes</td><td>Yes</td><td>Yes</td><td>Yes</td><td>Yes</td></tr>
</table>

4. Experimental Verification

4.1. Stimulated Brillouin Scattering

As depicted in Figure 8, we compared the calculated threshold powers for generating Brillouin scattering with experimental results. These experimental results include values from the published literature as well as our own measurements. The threshold powers for Brillouin scattering in optical fibers with lengths of 1 km, 2 km, 3 km, and 4 km are obtained from ref. [34]. For optical fiber lengths ranging from 5 km to 17 km, we cite the measured threshold powers from ref. [35]. In our laboratory, we conducted experiments using a 120 km single mode fiber to determine the threshold power for generating Brillouin scattering. Our experimental results indicate that the threshold power for a 120 km length optical fiber is approximately 8 mW.

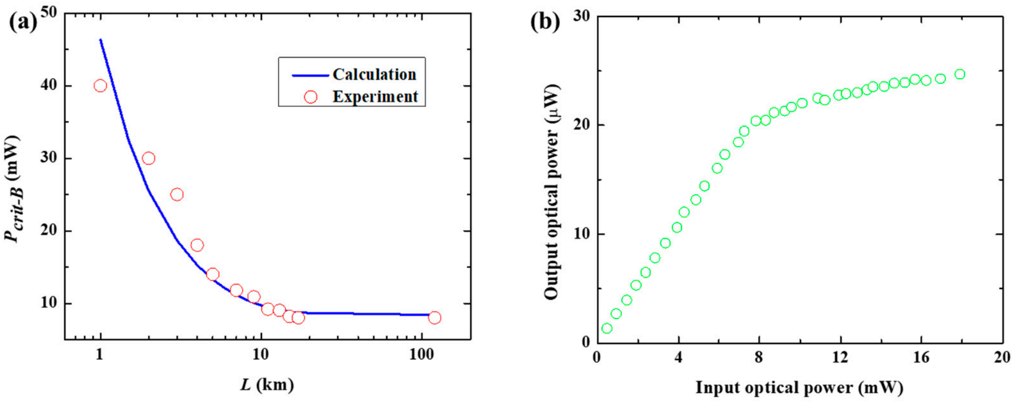

Figure 8. Comparison of calculated and experimental values of the threshold power for generating the Brillouin scattering. The attenuation coefficient α and the effective mode area A_{eff} are 0.2 dB/km and 1.0×10^{-10} m^2, respectively. The gain coefficient γ_B of the Brillouin scattering is 5.0×10^{-11} m/W. (**a**) Comparison of calculated and experimental values of the threshold power for generating the Brillouin scattering as a function of the optical fiber length L. (**b**) The experimental measurement results of the input optical power and the output optical power when the fiber length is 120 km.

Overall, the calculated threshold powers for generating Brillouin scattering align well with the experimental measurements. On average, there is a difference of about 4.5% between the experimental and calculated values. The largest discrepancy, about 34%, is observed at a fiber length of 3 km, while the smallest difference of approximately 1% is observed at a length of 13 km. Notably, for fiber lengths ranging from 2 km to 7 km, the experimental threshold powers for generating Brillouin scattering are higher than the calculated values. However, for fiber lengths ranging from 11 km to 120 km, the experimental results are lower than the calculated values. For instance, at a fiber length of 2 km, the experimental and calculated threshold powers for generating Brillouin scattering are approximately 30 mW and 25.5 mW, respectively. The experimental results show that the threshold powers for generating Brillouin scattering are approximately 9.2 mW, which is slightly higher than the calculated values. This experiment is conducted using an optical fiber length of 11 km.

4.2. Raman Scattering

As shown in Figure 9, we compare the calculated results with the experimental results of the threshold power for generating the Raman scattering, including the threshold power $P_{crit-R-F}$ for forward Raman scattering and the threshold power $P_{crit-R-B}$ for backward Raman scattering. The experimental results of the threshold power for generating the Raman scattering are cited in ref. [36].

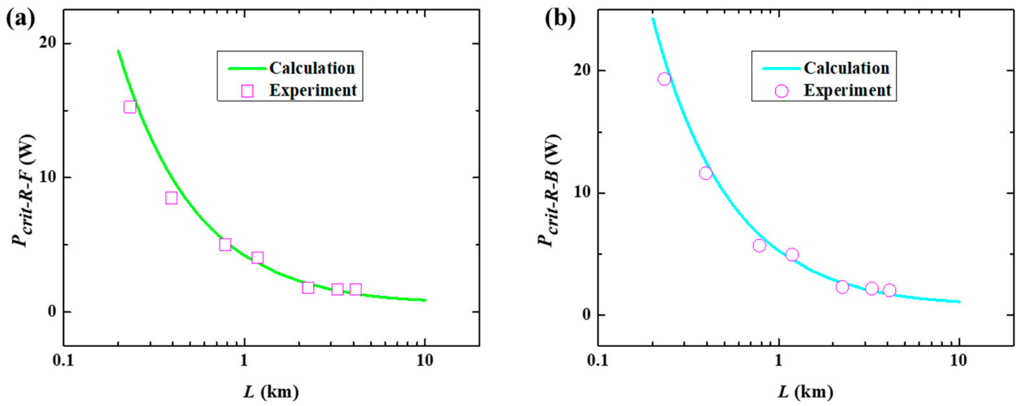

Figure 9. Comparison of calculated and experimental values of the threshold power for generating the Raman scattering. The attenuation coefficient α and the effective mode area A_{eff} are 0.2 dB/km and 1.0×10^{-10} m^2, respectively. The gain coefficient γ_R of the Brillouin scattering is 4.2×10^{-13} m/W. (**a**) Comparison of calculated and experimental values of the threshold power for generating the forward Raman scattering as a function of the optical fiber length L. (**b**) Comparison of calculated and experimental values of the threshold power for generating the backward Raman scattering as a function of the optical fiber length L.

The threshold power $P_{crit-R-F}$ for forward Raman scattering is investigated. The experimental and calculated values show good agreement, with an overall difference of approximately 10%. Notably, the largest difference between the calculated and experimental values is observed at a fiber length of 2.2 km, reaching about 22%. Conversely, the smallest difference is observed at a fiber length of 3.2 km, which is approximately 0.3%. Additionally, for fiber lengths ranging from 0.2 km to 0.8 km, the calculated value exceeds the experimental value. However, at fiber lengths of 1.1 km and 4.1 km, the calculated value is lower than the experimental value. For instance, at a fiber length of 0.2 km, the experimental and calculated values are approximately 14.3 W and 16.9 W, respectively. When the fiber length is 4.1 km, the experimental value and calculated value are about 1.7 W and 1.4 W, respectively.

The experimental results and calculated values for the threshold power $P_{crit-R-B}$ for backward Raman scattering show good agreement, which is similar to the threshold power $P_{crit-R-F}$. Generally, the difference between the experimental results and calculated values of $P_{crit-R-B}$ is approximately 2% lower than that of $P_{crit-R-F}$. When the fiber length is 2.2 km, the difference between the calculated value and the experimental value is the largest (around 20.6%). On the other hand, when the fiber length is 3.2 km, the difference between the calculated value and the experimental value is the smallest (approximately 2.5%). These two points resemble the behavior observed in the threshold power $P_{crit-R-F}$. Additionally, when the fiber length ranges from 0.2 km to 0.8 km, the experimental value is lower than the calculated value. However, for fiber lengths of 3.3 km and 4.1 km, the calculated value is lower than the experimental value. For instance, at a fiber length of 0.8 km, the experimental value and calculated value are approximately 5.7 W and 6.6 W, respectively. Similarly, at a fiber length of 4.1 km, the experimental value and calculated value are approximately 2.0 W and 1.7 W, respectively.

Through the experimental method, researchers have investigated the effects of various parameters on the threshold power for generating Brillouin scattering and Raman scattering [34–40]. These parameters include optical fiber length [34–36,40], input pump powers [38], and special types of optical fibers, such as photonic crystal fiber [39] and three-layer fiber [37]. For example, R. Parvizi et al. conducted a study on the threshold power for generating Brillouin scattering in photonic crystal fiber. They propose an approach to calculate this threshold and find that their results align well with experimental and simulation data. Similarly, E.B. Mejía et al. [39] examine the threshold power for generating Raman scattering as a function of doped-fiber length (specifically, lengths lower than approximately 1.3 m). Their experimental results demonstrate good agreement between the measured and calculated threshold powers for both backward and forward Raman scattering.

5. Conclusions

In this work, nonlinear effects in optical fiber frequency transfer are investigated through theoretical and simulation calculations in detail. We focus on the main nonlinear effects, including the Brillouin scattering and the Raman scattering. Generally, the threshold power of the Brillouin scattering is two orders lower than that of the Raman scattering. The calculation results show that the threshold powers of the Brillouin scattering and the Raman scattering decrease with the increase in the fiber length; however, the threshold powers basically do not change with the fiber length when the fiber length is greater than 10 km. When the length L of the fiber is constant, the threshold power of the Brillouin scattering and the Raman scattering decreases as the gain coefficients increase. However, for the attenuation coefficient α, the results are the opposite. In addition, when the fiber length L is determined and the linewidth Δv_{laser} of the laser source is from 1 Hz to 1 MHz, the linewidth Δv_{laser} of the laser source does not affect the threshold powers of generating the Brillouin scattering. As far as we know, this work is the first time to investigate nonlinear effects in optical fiber frequency transfer in detail. This work aims to provide reference design guidance for the reduction of nonlinear effects in optical fiber frequency transfer. The calculation result has potential guiding significance for many applications using Brillouin and Raman scattering characteristics, such as laser and optical fiber sensing. In future research, we will primarily focus on studying the nonlinear effects of optical fibers with lengths exceeding 500 km, as well as field optical fibers and special optical fibers, in the context of optical fiber frequency transfer.

Author Contributions: Conceptualization, G.X. and J.G.; methodology, D.J. and X.Z.; software, J.G.; validation, D.J. and J.B.; investigation, G.X. and M.W.; data curation, J.G.; writing—original draft preparation, G.X.; writing—review and editing, G.X. and J.G.; visualization, L.Z. and Q.Z.; supervision, R.D.; project administration, T.L. and S.Z. All authors have read and agreed to the published version of the manuscript.

Funding: The project is partially supported by the Chinese National Natural Science Foundation (Grant No. 12303076 and 11903041), the Youth Innovation Promotion Association of the Chinese Academy of Sciences, and the Young Innovative Talents of the National Time Service Center of the Chinese Academy of Sciences (Grant No. Y917SC1).

Institutional Review Board Statement: Not applicable.

Informed Consent Statement: Not applicable.

Data Availability Statement: The data presented in this study are available on request from the corresponding author. The data are not publicly available due to the data also being part of an ongoing study.

Conflicts of Interest: The authors declare no conflict of interest.

References

1. Marti, G.E.; Hutson, R.B.; Goban, A.; Campbell, S.L.; Poli, N.; Ye, J. Imaging Optical Frequencies with 100 μHz Precision and 1.1 μm Resolution. *Phys. Rev. Lett.* **2018**, *120*, 103201. [CrossRef] [PubMed]
2. Schioppo, M.; Brown, R.C.; McGrew, W.F.; Hinkley, N.; Fasano, R.J.; Beloy, K.; Yoon, T.; Milani, G.; Nicolodi, D.; Sherman, J.A.; et al. Ultra-stable optical clock with two cold-atom ensembles. *Nat. Photonics* **2017**, *11*, 48. [CrossRef]
3. McGrew, W.F.; Zhang, X.; Fasano, R.J.; Schaffer, S.A.; Beloy, K.; Nicolodi, D.; Brown, R.C.; Hinkley, N.; Milani, G.; Schioppo, M.; et al. Faraday-Shielded dc Stark-Shift-Free Optical Lattice Clock. *Nature* **2018**, *564*, 87. [CrossRef]
4. Lisdat, C.; Grosche, G.; Quintin, N.; Shi, C.; Raupach, S.; Grebing, C.; Nicolodi, D.; Stefani, F.; Al-Masoudi, A.; Dorscher, S.; et al. A clock network for geodesy and fundamental science. *Nat. Commun.* **2016**, *7*, 12443. [CrossRef]
5. Hu, L.; Poli, N.; Salvi, L.; Tino, G.M. Atom interferometry with the Sr optical clock transition. *Phys. Rev. Lett.* **2017**, *119*, 263601. [CrossRef]

6. Grotti, J.; Koller, S.; Vogt, S.; Häfner, S.; Sterr, U.; Lisdat, C.; Denker, H.; Voigt, C.; Timmen, L.; Rolland, A.; et al. Geodesy and metrology with a transportable optical clock. *Nat. Phys.* **2018**, *14*, 437. [CrossRef]
7. Droste, S.; Ozimek, F.; Udem, T.; Predehl, K.; Hänsch, T.W.; Schnatz, H.; Grosche, G.; Holzwarth, R. Optical Frequency Transfer over a single-span 1840 km Fiber Link. *Phys. Rev. Lett.* **2013**, *111*, 110801. [CrossRef]
8. Chiodo, N.; Quintin, N.; Stefani, F.; Wiotte, F.; Camisard, E.; Chardonnet, C.; Santarelli, G.; Amy-Klein, A.; Pottie, P.E.; Lopez, O. Cascaded optical fiber link using the Internet network for remote clocks comparison. *Opt. Express* **2015**, *23*, 33927. [CrossRef]
9. Deng, X.; Liu, J.; Jiao, D.D.; Gao, J.; Zang, Q.; Xu, G.J.; Dong, R.F.; Liu, T.; Zhang, S.G. Coherent Transfer of Optical Frequency over 112 km with Instability at the 10^{-20} Level. *Chin. Phys. Lett.* **2016**, *33*, 114202. [CrossRef]
10. Husmann, D.; Bernier, L.G.; Bertrand, M.; Calonico, D.; Chaloulos, K.; Clausen, G.; Clivati, C.; Faist, J.; Heiri, E.; Hollenstein, U.; et al. SI-traceable frequency dissemination at 1572 nm in a stabilized fiber network with ring topology. *Opt. Express* **2021**, *29*, 24592. [CrossRef]
11. Jiang, H. Development of Ultra-Narrow-Linewidth Laser Sources and Long-Distance Optical Link via Telecommunication Networks. Ph.D. Thesis, Université Paris, Paris, France, 2010.
12. Zang, Q. Key Techniques Research on Long-Haul Optical Frequency Transfer via Fiber Link. Ph.D. Thesis, University of Chinese Academy of Sciences, Beijing, China, 2022.
13. Deng, X. Research on High-Precision Optical Frequency Transfer via Fiber Link. Ph.D. Thesis, University of Chinese Academy of Sciences, Beijing, China, 2020.
14. Terra, O.; Grosche, G.; Schnatz, H. Brillouin amplification in phase coherent transfer of optical frequencies over 480 km fiber. *Opt. Express* **2010**, *18*, 016102. [CrossRef]
15. Grosche, G.; Terra, O.; Predehl, K.; Holzwarth, R.; Lipphardt, B.; Vogt, F.; Sterr, U.; Schnatz, H. Optical frequency transfer via 146 km fiber link with 10^{-19} relative accuracy. *Opt. Lett.* **2009**, *34*, 2270. [CrossRef] [PubMed]
16. Predehl, K.; Grosche, G.; Raupach, S.M.F.; Droste, S.; Terra, O.; Alnis, J.; Legero, T.; Hänsch, T.W.; Udem, T.; Holzwarth, R.; et al. A 920-Kilometer Optical Fiber Link for Frequency Metrology at the 19th Decimal Place. *Science* **2012**, *336*, 441–444. [CrossRef] [PubMed]
17. Predehl, K. A 920 km Optical Fiber Link for Frequency Metrology at the 19th Decimal Place. Ph.D. Thesis, Max-Planck-Institut für Quantenoptik, München, Germany, 2012.
18. Williams, P.A.; Swann, W.C.; Newbury, N.R. High-stability transfer of an optical frequency over long fiber-optic links. *J. Opt. Soc. Am. B* **2008**, *25*, 1284–1293. [CrossRef]
19. Koyamada, Y.; Sato, S.; Nakamura, S.; Sotobayashi, H.; Chujo, W. Simulating and designing Brillouin gain spectrum in single mode fibers. *J. Light. Technol.* **2004**, *22*, 631. [CrossRef]
20. McCurdy, A.H. Modeling of stimulated Brillouin scattering in optical fibers with arbitrary radial index profile. *J. Light. Technol.* **2005**, *23*, 3509. [CrossRef]
21. Okawachi, Y. Tunable all-optical delays via Brillouin slow light in an optical fiber. *Phys. Rev. Lett.* **2005**, *94*, 153902. [CrossRef]
22. Ward, B.; Spring, J. Finite element analysis of Brillouin gain in SBS-suppressing optical fibers with non-uniform acoustic velocity profiles. *Opt. Express* **2009**, *17*, 15685. [CrossRef]
23. Kovalev, V.I.; Harrison, R.G. Suppression of stimulated Brillouin scattering in high-power single-frequency fiber amplifiers. *Opt. Lett.* **2006**, *31*, 161. [CrossRef]
24. Agrawal, G.P. *Nonlinear Fiber Optics*, 4th ed.; Academic Press: New York, NY, USA, 2007.
25. Kovalev, V.I.; Harrison, R.G. Abnormally low threshold gain of stimulated Brillouin scattering in long optical fiber with feedback. *Opt. Express* **2008**, *16*, 12272. [CrossRef]
26. Cao, M.; Li, H.; Tang, M.; Mi, Y.; Ren, G. Forward stimulated Brillouin scattering in optical nanofibers. *J. Opt. Soc. Am. B* **2019**, *36*, 2079. [CrossRef]
27. Serena, P.; Meseguer, A.C.; Poli, F.; Bononi, A.; Antona, J.C. Scaling properties of guided acoustic-wave Brillouin scattering in single-mode fibers. *Opt. Express* **2021**, *29*, 15528. [CrossRef] [PubMed]
28. Wolff, C.; Smith, M.; Stiller, B.; Poulton, C. Brillouin scattering—Theory and experiment: Tutorial. *J. Opt. Soc. Am. B* **2021**, *38*, 1243. [CrossRef]
29. Nieves, O.A.; Arnold, M.D.; Steel, M.J.; Schmidt, M.K.; Poulton, C.G. Numerical simulation of noise in pulsed Brillouin scattering. *J. Opt. Soc. Am. B* **2021**, *38*, 2343. [CrossRef]
30. Jin, D.; Bai, Z.; Lu, Z.; Fan, R.; Zhao, Z.; Yang, X.; Wang, Y.; Mildren, R.P. 22.5-W narrow-linewidth diamond Brillouin laser at 1064 nm. *Opt. Lett.* **2022**, *47*, 5360–5363. [CrossRef] [PubMed]
31. Miah, K.; Potter, D.K. A Review of Hybrid Fiber-Optic Distributed Simultaneous Vibration and Temperature Sensing Technology and Its Geophysical Applications. *Sensors* **2017**, *17*, 2511. [CrossRef]
32. Ippen, E.P.; Stolen, R.H. Stimulated Brillouin scattering in optical fibers. *Appl. Phys. Lett.* **1972**, *21*, 539. [CrossRef]
33. Smith, R.G. Optical power handling capacity of low loss optical fibers as determined by stimulated Raman and Brillouin scattering. *Appl. Opt.* **1972**, *11*, 2489. [CrossRef]
34. Al-Asadi, H.A.; Al-Mansoori, M.H.; Hitam, S.; Saripan, M.I.; Mahdi, M.A. Particle swarm optimization on threshold exponential gain of stimulated Brillouin scattering in single mode fibers. *Opt. Express* **2011**, *19*, 1842–1853. [CrossRef]
35. Al-Asadi, H.A.; Al-Mansoori, M.H.; Ajiya, M.; Hitam, S.; Saripan, M.I.; Mahdi, M.A. Effects of pump recycling technique on stimulated Brillouin scattering threshold: A theoretical model. *Opt. Express* **2010**, *18*, 22339–22347. [CrossRef]

36. Yang, Y.; Yang, W.; Jiang, T.; Yang, M. Investigation characteristics of stimulated Raman Threshold in a Single Mode Fiber. *Acta Opt. Sin.* **2014**, *34*, 129001. [CrossRef]
37. Khudyakov, M.M.; Likhachev, M.E.; Bubnov, M.M.; Lipatov, D.S.; Lobanov, A.S.; Guryanov, A.N. Three layer fiber with high stimulated Brillouin scattering threshold. In Proceedings of the Fiber Lasers XIV: Technology and Systems, San Francisco, CA, USA, 28 January–2 February 2017; Volume 10083.
38. Parvizi, R.; Harun, S.W.; Ali, N.M.; Arof, H.; Ahmad, H. Investigation on threshold power of stimulated Brillouin scattering in photonic crystal fiber. *Optik* **2012**, *123*, 1149–1152. [CrossRef]
39. Mejía, E.B.; De la Cruz May, L.; Talavera, D.V. Shortening of a Raman fiber laser by inserting ytterbium doped fiber. *IOSR J. Eng.* **2013**, *3*, 38–43. [CrossRef]
40. Liu, A.; Chen, X.; Li, M.J.; Wang, J.; Walton, D.T.; Zenteno, L.A. Comprehensive Modeling of Single Frequency Fiber Amplifiers for Mitigating Stimulated Brillouin Scattering. *J. Light. Technol.* **2009**, *27*, 2189–2198.